

# A GPU-Based Grid Traverse Algorithm for Accelerating Lightning Geolocation Process

Zilong Qin, *Member, IEEE*, Mingli Chen , Fanchao Lyu , *Member, IEEE*, Steven A. Cummer, *Fellow, IEEE*, Baoyou Zhu, Feifan Liu, and Yaping Du 

**Abstract**—Most lightning location networks are based on real-time analytical solutions of certain simplified models, while the reality is much more complicated. In this paper, we introduce a graphics processing unit (GPU)-based parallel computing algorithm that can extensively benefit lightning geolocation networks. For a network running this GPU-based algorithm, one can build up a geolocation database based on numerical solutions of certain complete models in advance, and lightning geolocations can then be easily determined with a grid-searching technique in real time. One such grid-searching technique, is the grid traverse algorithm (GTA) for the traditional time of arrival technique. By running GPU-based GTA in a six-station two-dimensional (2-D) and a five-station 3-D networks, we show that extremely high network performance can be achieved, with a processing speed of about 2700 times faster than CPU-based GTA. The location accuracy of GPU-GTA is examined with Monte Carlo simulations, showing that GPU-GTA can locate a lightning source in real time with high accuracy. We also find that when the grid step is comparable with the inherent time uncertainty of a network, the location accuracy cannot be improved further with a finer grid step.

**Index Terms**—Graphics processing unit (GPU)-based computing algorithm, lightning electromagnetic pulse, lightning source location, time of arrival (TOA) technique.

## I. INTRODUCTION

**L**IGHTNING locations from ground-based lightning location networks provide fundamental information for scientific researches as well as the society of meteorology. Either in a long-baseline two-dimensional (2-D) lightning location network [1]–[16] or in a 3-D lightning mapping array (LMA) [17]–[28], the geolocation algorithm is always a critical technique

to operate the network. Generally, there are three basic lightning geolocation techniques or their combinations that were deployed in existing networks. They are the time of arrival (TOA) technique [29], the magnetic direction finder (MDF) technique [30], and the interferometric direction-finding technique, as well as their combination [31]. In a long-baseline lightning location network operating essentially in extremely low-frequency (ELF)/very low-frequency (VLF) bands, the time of group arrival (TOGA) technique is preferred [5], [32]. The interferometric direction-finding technique is widely used in 2-D short-baseline VHF interferometry systems [33]–[43]. The TOA technique is the basic method for most of the 3-D LMAs operating either in VHF or LF bands [17]–[25], whereas the interferometric direction-finding technique is also adopted in many 3-D LMAs [26]–[28]. The TOA technique finds the source location by matching the signal arrival time differences for each pair of sensors. For every two sensors (forming a baseline), the solution satisfying the TOAs to these two sensors will form a parabolic curve. By adding another proper baseline (another sensor), the source location that matches the arrival time differences of all baselines is the intersection point of the two parabolic curves. If the baselines are much shorter than the distances to the lightning source, finding the intersection point of the two parabolic curves becomes finding the direction of the line coinciding the two parabolic curves, which is the interferometric direction-finding technique. The TOGA technique estimates the lightning source distance by measuring the group delays of frequencies of lightning sferics above the cut-off frequency of the earth-ionosphere waveguide (EIWG). The MDF technique identifies the source location by deploying the intersection of at least two azimuthal lines, each of which can be retrieved by orthogonal magnetic field measurements.

The lightning location based on the TOA technique can be solved with Chan's algorithm without iteration if the earth curvature is ignorable. When the earth curvature has to be considered, it turns to a nonlinear optimization problem. The conventional method to tackle this kind of nonlinear problem is to use the gradient search technique (e.g. Levenberg–Marquart and Newton–Raphson methods) [9], [29], whose initial value of the search is often estimated from Chan's algorithm with no consideration of the earth curvature. Besides, there are also some TOA networks that adopt the CPU-based numerical grid traverse algorithm (GTA). Differing from the iteration algorithm, the GTA builds a grid database first and then finds the grid point that matches the time differences [17], [44]. Although computing

Manuscript received October 20, 2018; revised February 25, 2019; accepted March 16, 2019. This work was supported in part by Research Grant Council of Hong Kong Government under Grant PolyU152652/16E. (*Corresponding author: Mingli Chen.*)

Z. Qin, M. Chen, F. Lyu, and Y. Du are with the Department of Building Service Engineering, The Hong Kong Polytechnic University, Hong Kong (e-mail: zilong.qin@connect.polyu.hk; mingli.chen@polyu.edu.hk; fanchao.lyu@gmail.com; ya-ping.du@polyu.edu.hk).

S. A. Cummer is with the Department of Electrical and Computer Engineering, Duke University, Durham, NC 27708 USA (e-mail: cummer@duke.edu).

B. Zhu and F. Liu are with the CAS Key Laboratory of Geospace Environment, School of Earth and Space Sciences, University of Science and Technology of China, Hefei 230022, China (e-mail: zhuby@ustc.edu.cn; lff@mail.ustc.edu.cn).

Color versions of one or more of the figures in this paper are available online at <http://ieeexplore.ieee.org>.

Digital Object Identifier 10.1109/TEMC.2019.2907715

burdensome, the GTA has some advantages. It is much simpler than the iteration method, which does not need an initial value and is inherently accurate. Specifically, for radio geolocation applications, delays of radio wave propagation due to the earth topography can be considered in GTA to improve the geolocation accuracy. The earth topography has significant influences on the propagation of lightning electromagnetic waves, inducing the time uncertainty of TOA. In some networks, very sophisticated approaches for corrections of the sensor's site errors and the lightning field propagation time delays were adopted [45], [46]. Through quantitative estimation with finite-difference time domain (FDTD) wave modeling [47]–[49], time corrections for a given network can be obtained and easily inputted to the GTA database in advance, which can significantly improve the accuracy of the location network.

The CPU-based GTA algorithm usually has poor efficiency when extensive computing is needed, which limits its applications in real-time geolocation networks. With the development of graphics processing unit (GPU) parallel computing technique, numerical computations can be largely accelerated [50]. In this study, we propose a GPU-based GTA algorithm, which is simple for implementation and is more efficient than a CPU-based GTA algorithm. Its applications to a 2-D long-baseline network and a 3-D short-baseline network show that GPU-GTA can work efficiently and accurately in locating a lightning source in either 2-D or 3-D. The high performance of GPU-GTA makes it a practical algorithm for accurately locating a lightning source in real time.

## II. TOA LIGHTNING LOCATION AND GPU-BASED PARALLEL COMPUTING TECHNIQUE

The TOA algorithm determines the geolocation of lightning sources with the difference of TOA of electromagnetic field signals from the same source to different sensors. It has been widely applied to both 2-D [3] and 3-D [19] lightning networks. Theoretically, TOA geolocation networks need at least four sensors to obtain 2-D locations of the sources (latitude and longitude) and five sensors for 3-D locations (latitude, longitude, and altitude). Some redundant sensors are required to get more reliable source locations. For one baseline containing two sensors, the arrival time difference can be written as follows:

$$\Delta t = t_2 - t_1 \quad (1)$$

where  $t_1$  and  $t_2$  are the arrival times of the source waves measured at different sensors.  $\Delta t$  is the time difference between the two sensors, which can be measured taking the signal onset times, the windowed cross-correlation in broadband systems, or the phase difference in narrowband systems.

With multiple baselines, the solution of geolocation can be obtained by optimizing the objective function  $f(\mathbf{r})$  as follows

$$f(\mathbf{r}) = \sum_{i=1}^{N-1} |\Delta t_i - (\Delta t'_i(\mathbf{r}) + (\sigma_2 - \sigma_1))| \quad (2)$$

where  $N$  is the number of sensors,  $\sigma_{1,2}$  is the inherent propagation factors through each path, which can be pre-determined by the wave propagation modeling.  $\Delta t'_i$  is the propagation time difference from a source location  $\mathbf{r}$  to each sensor:  $\Delta t'_i(\mathbf{r}) = (d(\mathbf{r}, \mathbf{r}_i) - d(\mathbf{r}, \mathbf{r}_0))/c$ , where  $c$  is the speed

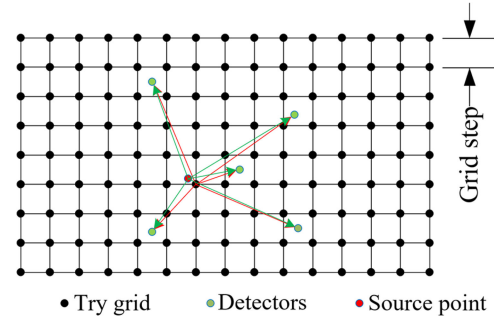


Fig. 1. Sketch map of GTA in a lightning location network. Where the detection region is separated evenly in grid. Red point is the location of a lightning source; green points are the locations of sensors; and black points are the try locations in each grid.

of light and  $d(\mathbf{r}, \mathbf{r}_i)$  the distance along the propagating path. For a short-baseline network around 5–50 km,  $d(\mathbf{r}, \mathbf{r}_i)$  is usually defined as the straight distance between the source and the sensor [17]–[25]. For a short-baseline network like the Vaisala system, electromagnetic field signals from lightning emission sources propagate along the earth surface, and therefore,  $d(\mathbf{r}, \mathbf{r}_i)$  is defined as the spherical distance between the source and the sensor [1]–[4], [6]–[16]. For long-baseline network (above 3000 km), which essentially uses the ELF and VLF bands, (2) is only suitable for signals with frequencies below the EIWG cut-off frequency (usually below 2 kHz, differs during day and night time). For frequencies above the EIWG cut-off frequency, the TOGA method taking account of the effects of the dispersion of the EIWG on the lightning sferics is much more preferred [32]. The conventional method solves the nonlinear iteration (2) directly (the 3D iteration solver of (2) can be found in [29]) to find a solution, whereas the GTA traverses prebuilt, discretized grids of the network region to find the best-fitted solution that has the smallest  $f(\mathbf{r})$ . It is straightforward but computing costly, and thus its overall performance, such as the speed and locating precision, relies heavily on the grid step and the network coverage.

A sketch map of a prebuilt discretized 2-D region is shown in Fig. 1. As illustrated in the figure, by computing  $f(\mathbf{r})$  at each grid, the best-fitted source location can be retrieved by finding the grid having the smallest  $f(\mathbf{r})$ .

### A. Traditional GTA With/Without Parallel Computing

The traditional CPU-based GTA (CPU-GTA) calculates the at each point, comparing them one by one and remaining the point that has the smaller  $f(\mathbf{r})$ , with the whole process being entirely in a serial way. The performance is rather poor when the detection region is large, and the grid step is small. Considering a 2-D location situation, when the region is 1000 km south-north, and 1000 km east-west and the grid step is 250 m, a total of  $4000 * 4000 = 16$  million;  $f(\mathbf{r})$ s must be compared with each other in one geolocating process, which is almost impossible for a real-time system.

Fortunately, the GPU parallel computing technique provides a solution to accelerate the GTA process. GPU, which is designed on single instruction, multiple data architecture, contains an array of streamer multiprocessors (SM). Each

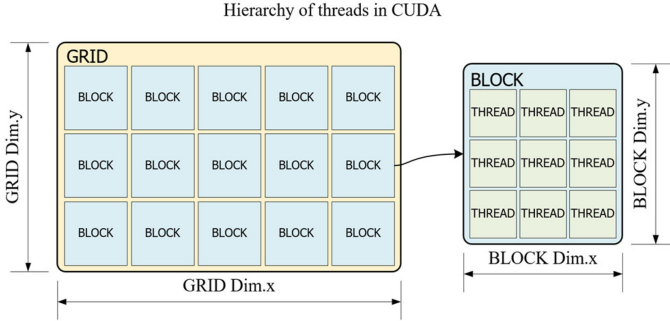


Fig. 2. Illustration of the thread hierarchy of CUDA programming model. The GRID consists of a 2- or 3-D matrix of BLOCKs, and each BLOCK consists of parallel THREADs. For specified GRID and BLOCK dimensions and a collective kernel function, the program runs in parallel for all THREADs.

SM has a large number of arithmetic logic units (ALUs) with only one control unit. All ALUs in one SM run the same instruction synchronously. The unique configuration of GPU makes it inherently conducive to numerical computing. Taking the lightning geolocation as an example, when applying GPU parallel computing to TOA technique, each ALU will run as one parallel thread to calculate one  $f(\mathbf{r})$ . All threads have the same function to run but with different data streams. Once all  $f(\mathbf{r})$ s are calculated, a reduction algorithm can be invoked to find the smallest  $f(\mathbf{r})$  in a parallel manner.

### B. CUDA Programming Model

CUDA is a general-purpose parallel computing platform that utilizes GPU to solve a large-scale parallel problem. CUDA was first introduced by NVIDIA in 2006 [51] and is now widely used in parallel scientific computing scenarios. It provides a high-level model to program GPU-based parallel applications. Below is a briefing of the hierarchy of CUDA. CUDA provides a three-level hierarchy to configure and invoke threads running on GPU, i.e., GRID, BLOCK, and THREAD.

Fig. 2 illustrates of the three-level hierarchy of the CUDA programming model. As shown in the figure, the GRID consists of BLOCKs, and each BLOCK consists of many THREADs. The dimension of the GRID and BLOCK can be 2 or 3. Once all model arguments are transferred, a kernel function will then be run on all threads with a specified GRID and BLOCK dimensions. In geolocation applications, GRID points are assigned to each THREAD, which has the same kernel function for calculating  $f(\mathbf{r})$  as (2), but with different arguments (i.e., latitude, longitude, and altitude at each point).

### C. Optimal Parallel Reduction Algorithm in CUDA

The final step in GTA is to find the point that has the smallest  $f(\mathbf{r})$ . This kind of job can only be run sequentially on a CPU-based platform. Even on a GPU-based parallel architecture, all threads cannot compare their  $f(\mathbf{r})$ s concurrently. Therefore, a parallel reduction algorithm is necessary for the optimization of this job [52].

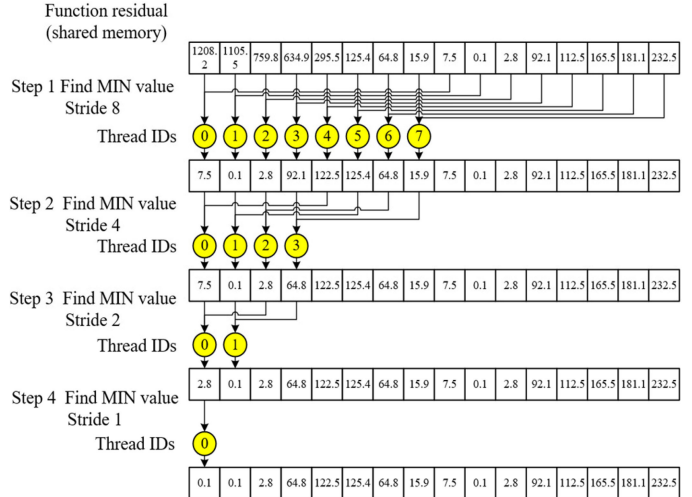


Fig. 3. Sketch map of parallel reduction algorithm on picking out the smallest  $f(\mathbf{r})$ . In a recursive structure, in each step, all threads are divided into two equal groups, each thread in group A compares its  $f(\mathbf{r})$  with one in group B, transferring the smaller  $f(\mathbf{r})$  to group A and discarding the thread in group B. After a thread synchronization, all group A threads then go to the next run until only one residual thread left in group A.

Fig. 3 shows a sketch map illustrating the parallel reduction algorithm. As shown in the figure, the output from every two threads in one step are compared and the one with smaller  $f(\mathbf{r})$  is swapped forward in each thread. In this way, the smallest one will be quickly converged to the first thread in a few steps. The stride between the two competitors in each step is  $N/2^i$ , where  $N$  is the amount of total grid points in a lightning location network and  $i$  is the index number of the step. As such, the smallest  $f(\mathbf{r})$  will be quickly shifted to the first thread in a loop index of  $\log_2 N$ , which leads to the final location result. More details of the parallel reduction algorithm can be found in [52].

### D. GPU-GTA for 3-D Lightning Location

The GPU-GTA algorithm can be easily extended to a 3-D lightning location network or any other coordinates that have a describable objective function. For a 3-D location, it needs to introduce a new argument—altitude  $h$

$$d(\mathbf{r}, \mathbf{r}_i) = \sqrt{(R(1 - \cos(\theta)) + h)^2 + (R \sin(\theta))^2}. \quad (3)$$

Here the earth curvature is considered. Where  $\theta$  is the arc length between the two points,  $R$  is the earth radius or the local radius in an ellipsoidal coordinate, and  $h$  is the altitude.

### E. Multi-Grid Traverse Technique

A 3-D geolocation domain usually has a large number of grid points. If the grid amount is extremely large, like the traditional GTA, a multi-grid traverse technique can be introduced to further speed up the GPU-GTA process. The multi-grid traverse technique can be applied at least twice in a traverse to find the final solution. It first traverses the whole region with a rough

grid step to find an initial result and then traverses a small region centered at the initial result with a finer grid to retrieve the final solution.

### III. VALIDATION OF GPU-GTA WITH MONTE CARLO SIMULATION FOR VARIOUS NETWORKS

In this section, we validate the GPU-GTA algorithm by implementing Monte Carlo simulations of geolocation errors in different sorts of lightning networks [9]. In the simulation, random time errors are introduced to true arrival times in the geolocation algorithm and possible location error patterns are estimated by comparing the GPU-GTA location results with the true locations. This is the basic idea to understand the accuracy of a lightning location network or test the location algorithm. For doing this, first, a Gaussian distributed time error is applied to each true arrival time from each pre-built location point to each sensor in a given lightning location network. Second, the “deviated” arrival times are input into the GPU-GTA or CPU-GTA to calculate the locations with errors. Third, the calculated locations and their pre-built locations are compared to find the location errors (the distance differences between the two sets of locations). Then, the spatial pattern of the location errors in the region covered by the location network is obtained by averaging the location errors from at least 50 times of simulations. Finally, the performance of GPU-GTA and that of CPU-GTA are compared, and thus a benchmark to the GPU-GTA algorithm is given. The initial pre-built location at each point is randomly generated.

#### A. For a Long-Baseline 2-D Lightning Location Network

To test GPU-GTA in a 2-D location case, the network operated by the University of Science and Technology of China is chosen [6], [44]. This network was first deployed in 2012 in Anhui province over East China, with an upgrade conducted in 2015, which has been named as JASA network since then. The network was specially designed for lower ionosphere remote sensing [53]–[55], and the GPU-GTA is already running in this network, which yielded good data revealing the association of the Narrow Bipolar Events with and the Blue Jets [56].

JASA consists of six sensors, as illustrated in Fig. 4. Its coverage is  $1000 \text{ km} \times 1000 \text{ km}^2$  from west to east and from south to north, and the grid searching step for running GPU-GTA is in two-level grids with the multi-grid technique. The first-level grid is  $512 \times 512$  with a grid step of 2 km. The second-level grid is  $512 \times 512$  with a grid step of 125 m, which is centered at the position estimated from the first-level grid. In conducting the Monte Carlo simulation of location errors, a  $1\text{-}\mu\text{s}$  rms Gaussian-distributed time error and a linear propagation delay of 100 km per  $1 \mu\text{s}$  [the  $\sigma$  in  $f(\mathbf{r})$ ] are introduced to each event arrival time at each sensor.

The location error pattern at each randomly generated location point is shown in Fig. 4. As shown in the figure, location errors of GPU-GTA are smaller than 0.5 km inside the inner polygon region of the network, indicating a high performance of GPU-GTA running on JASA in 2-D.

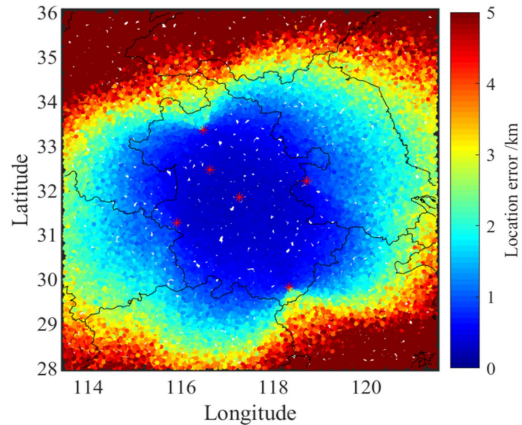


Fig. 4. Simulated location error pattern for JASA network running GPU-GTA with the Monte Carlo method. The JASA consists of six sensors separated over the area of central China, where the red asterisks indicate the six sensors. The color of each dot represents the averaged location error at each random location over the network covering region.

#### B. For a Short-Baseline 3-D LMA

To test GPU-GTA in a 3-D location case, the low-frequency interferometric-TOA LMA (LFI-LMA) run by Duke University during 2014 is chosen [17]. The LFI-LMA consists of five sensors separated by 15–20 km, as illustrated in Fig. 5. This portable network can be easily deployed to image the 3-D structure and dynamic development of lightning during thunderstorms [57].

Similar to a 2-D situation, with a  $0.1\text{-}\mu\text{s}$  rms Gaussian-distributed time error introduced to the true TOA, the location error patterns are obtained with the Monte Carlo simulation with GPU-GTA. It is implemented in a three-level grid approach, the first level is  $256 \times 256 \times 18$  grids with a step of 1 km, the second level is  $32 \times 32 \times 16$  with a step of 0.4 km, and the third level is  $128 \times 128 \times 120$  with a step of 25 m. The second level grid is centered at the position estimated from the first level one, and the third level grid is centered at the position estimated from the second level one. The results are shown in Fig. 5, where the horizontal (left) and vertical (right) location errors for the altitude of 5, 10, and 15 km are shown in subplots from top to bottom in the figure, respectively. As shown in the figure, the location error is much smaller at a higher altitude, with the error being less than 200 m over a much larger area at an altitude of 15 km. In a 3-D situation, since the solution surface of a baseline close to the ground tends to be tangential to the solution surface of another baseline, this may cause larger vertical uncertainty when close to the ground. The results show that LFI-LMA running GPU-GTA in 3-D can perform quite well, with the location errors being less than 200 m over most of the network coverage.

#### C. Location Accuracy of Networks Running GPU-GTA With Different Grid Steps

The geolocation accuracy is heavily subjected to the grid step used in GPU-GTA. Theoretically, if the grid step is finer enough, GPU-GTA can provide the ultimate location accuracy. However, a real lightning location system always has certain deviations

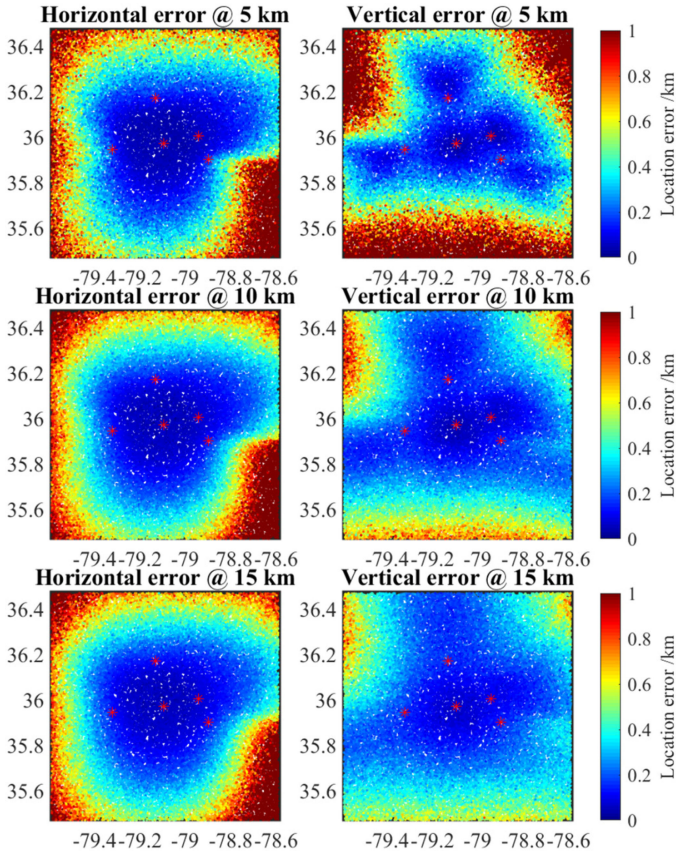


Fig. 5. Simulated location error patterns for Duke LFI-LMA network running the GPU-GTA algorithm with the Monte Carlo method. The LFI-LMA was consisted of five sensors separated by 15–20 km around Duke University, where the red asterisks indicate the five sensors' locations. The color of each dot represents the averaged location error at each random location over the network covering region. The top two subplots are for the horizontal (left) and vertical (right) errors for the altitude of 5 km, and the middle two and the bottom two for that of the altitude of 10 km and 15 km, respectively.

that limit the ultimate location accuracy the system can achieve. One such deviation is the time measuring the uncertainty of sensors in a network. It may come from the GPS timing uncertainty, data acquisition sampling rate, system operating bandwidth, signal-to-noise ratio as well as the method to extract the times from the recorded signals at different sensors. Although most of these factors are system hardware related, we just discuss the location accuracy versus the grid step under a fixed time uncertainty. This is particularly needed for finding the limitation of a network running GPU-GTA.

Fig. 6 shows the statistics of 2-D location errors in JASA running GPU-GTA with different grid steps, where a time uncertainty of  $1 \mu\text{s}$  rms is applied. As shown in the figure, considering the total number of points with location errors less than 500 m as a benchmark, it is 4174, 4684, and 4746 for the final grid step of 500, 250, and 125 m, respectively. From the grid step of 500–250 m, the number of highly accurate locations increases by 510 or 12%. But from the grid step of 250 m to 125 m, that number only increases by 62 or 1.3%. This property could be attributed to the  $1 \mu\text{s}$  rms time uncertainty introduced to each sensor, making the network with a location ambiguity between

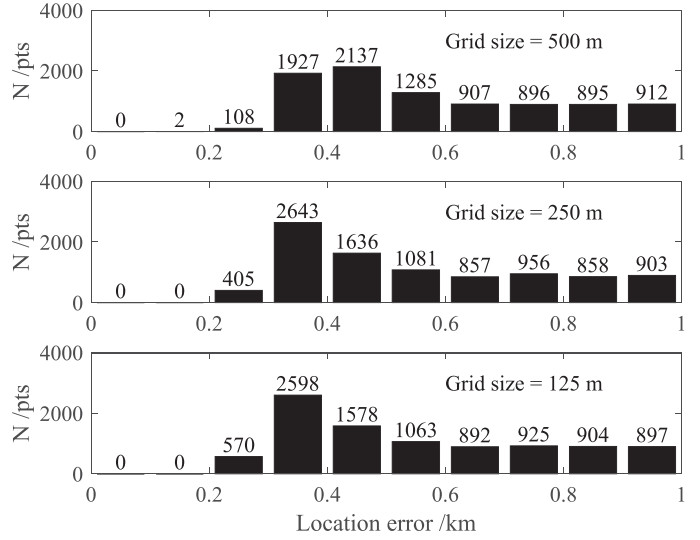


Fig. 6. Statistics of 2-D location errors in first 1 km of JASA running GPU-GTA with different grid steps and  $1 \mu\text{s}$  rms time uncertainty. The subplots from top to bottom are for the grid step of 500, 250, and 125 m respectively.

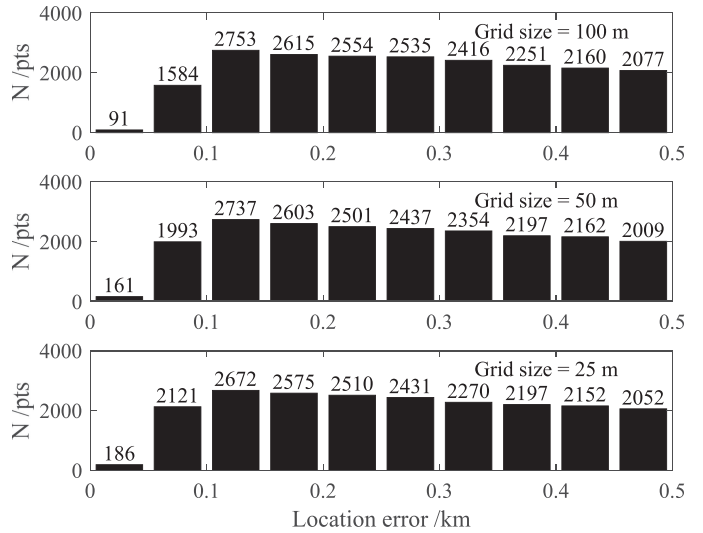


Fig. 7. Statistics of 3-D location errors in first 500 m of Duke LFI-LMA running GPU-GTA with different grid steps and  $0.1 \mu\text{s}$  rms time uncertainty at the altitude of 10 km. The subplots from top to bottom are for the grid step of 100, 50, and 25 m, respectively.

250 and 500 m. This suggests that 250 m may be the most economical grid step for JASA running GPU-GTA algorithm with a time uncertainty of  $1 \mu\text{s}$  rms, resulting in an ultimate location accuracy of about 250 m.

Fig. 7 shows the histogram of 3-D location errors of Duke LFI-LMA running GPU-GTA with different grid steps and  $0.1 \mu\text{s}$  rms time uncertainty at the altitude of 10 km. With the number of location point whose error is less than 100 m as a reference, when the grid step decreases from 100 m to 50 m, this number increases from 1675 to 2154, a big increase of 479 or 29%. However, when the grid step further decreases from 50 to 25 m, this number increases from 2154 to 2307, just an

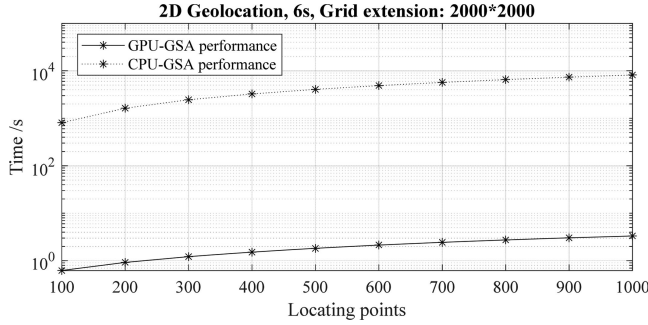


Fig. 8. Comparison of the processing time between the CPU-GTA and GPU-GTA for locating 100–1000 events in a three-sensor 2-D network with a grid extension of  $2000 \times 2000$ . Dotted line is for CPU-GTA and solid line is for GPU-GTA.

increase of 153 or 7%. This suggests that the most economical grid step for LFI-LMA running GPU-GTA algorithm with a time uncertainty of  $0.1 \mu\text{s rms}$  may be 50 m, resulting in an ultimate location accuracy of about 50 m.

Above-mentioned results indicate that GPU-GTA can work well with a reasonably high location accuracy in the inner region of either a 2-D network like JASA or a 3-D network like LFI-LMA. Also, the results show that the location accuracy is limited by the level of the inherent time uncertainty of the network, rather than the grid step if the grid step is small enough. GPU-GTA can give the ultimate accurate result when the grid step is suitable.

#### IV. PERFORMANCE OF GPU-GTA

The most significant merit of the GPU-GTA algorithm is that it can greatly increase the speed of computation compared with CPU-GTA. The processing speed is crucial to a lightning location network, especially for those built for real-time reporting. To have a quantitative evaluation of the GPU-GTA performance, we estimate the processing time for locating a certain number of events under a specific network with GPU-GTA and compare it with that of CPU-GTA.

Fig. 8 shows a comparison of the processing times between the CPU-GTA and GPU-GTA for locating 100–1000 lightning events in a 3-sensor 2D network with a grid extension of  $2000 \times 2000$ . Under such a configuration, locating one lightning event needs the GTA algorithm traversing all the 4 000 000 points. As can be seen from the figure, the GPU-GTA is generally 2700 times faster than the CPU-GTA under such a configuration.

Fig. 9 shows a comparison of the computing speeds of the GPU-GTA between three different setups of a two-level-grid traverse technique for a six-sensor 2-D network like JASA. In a two-level-grid traverse technique, the traversing process can start with a relatively big initial grid step (e.g., 2 km). Once an initial event position is acquired with the initial grid step, a finer grid step (e.g., 125 m) can be taken to traverse a small space centered at the initial position to get the accurate event position. In the figure, while the first-level grid is set at a step of 2 km with an extension of  $512 \times 512$ , the second-level grid is set at three different steps of 500, 250, and 125 m corresponding to three different extensions of  $128 \times 128$ ,  $256 \times 256$ , and  $512 \times 512$ , respectively.

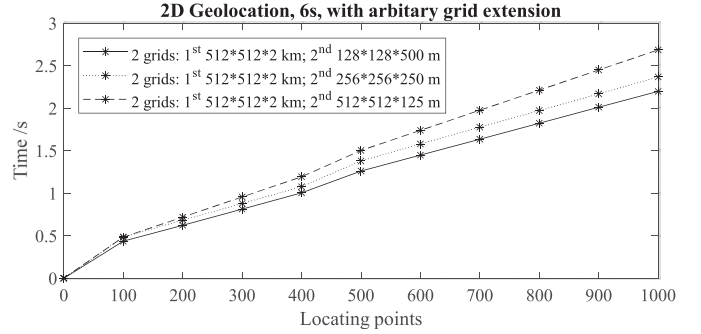


Fig. 9. Comparisons of processing times of GPU-GTA operated in a six-sensor 2-D network like JASA with three different sets of grid steps and extensions. While the first level grid is set with a grid step and an extension of 2 km and  $512 \times 512$ , the second level grid is set with three different grid steps/extensions of 500 m/ $128 \times 128$  (solid line), 250 m/ $256 \times 256$  (dotted line), and 125 m /  $512 \times 512$  (dashed line), respectively.

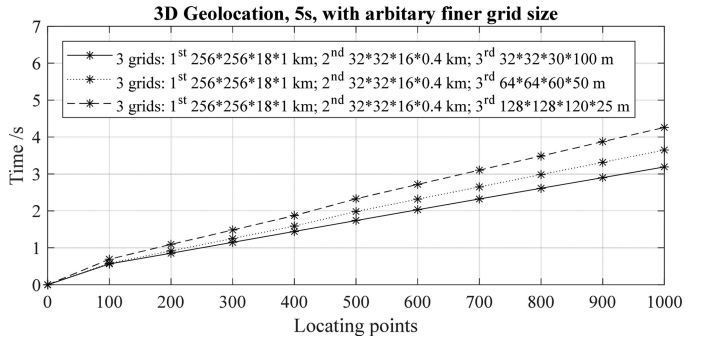


Fig. 10. Comparisons of processing times of GPU-GTA running in a five-sensor 3-D network like LFI-LMA with a three-level-grid traverse technique under three different grid step and extension settings. The first- and second-level grid steps are 1 km and 0.4 km with a grid extension of  $256 \times 256 \times 18$  and  $32 \times 32 \times 16$ , respectively. The third-level (final) grid is set with three different steps/extensions of 100 m/ $32 \times 32 \times 30$  (solid line), 50 m/ $64 \times 64 \times 60$  (dotted line) and 25 m/ $128 \times 128 \times 120$  (dashed line), respectively.

As can be seen from the figure, with the increase in the grid extension, the processing time increases linearly. It costs about 2.7 s to locate 1000 events in this 6-sensor network covering an area of  $1000 \text{ km} \times 1000 \text{ km}$  with the grid step of 125 m. Such a computing speed could be efficient enough for a real-time lightning network.

Similar to the 2-D case, the performance of GPU-GTA in a 3-D network is also evaluated.

Fig. 10 shows the processing times of GPU-GTA operated in a five-sensor 3-D network like LFI-LMA with a three-level-grid traverse technique with three different grid settings. The first-level (initial) grid is set with a step of 1000 m and an extension of  $120 \times 120 \times 18$ , corresponding to a cube of  $256 \text{ km} \times 256 \text{ km} \times 18 \text{ km}$  (altitude). The second-level grid is set with a step of 0.4 km and an extension of  $32 \times 32 \times 16$ . The third-level (final) grid is set with three different grid steps of 100, 50, and 25 m, respectively, with a grid extension of  $32 \times 32 \times 30$ ,  $64 \times 64 \times 60$ , and  $128 \times 128 \times 120$ , respectively, corresponding to a cube of  $3.2 \text{ km} \times 3.2 \text{ km} \times 3.2 \text{ km}$  centered at the position estimated from the second-level grid. As shown in the figure, it takes about 3.2, 3.6, and 4.3 s to

locate 1000 points in 3-D at the accuracy of 100, 50, and 25 m respectively. Again, the speed of GPU-GTA is efficient enough to satisfy a real-time 3-D lightning network like LFI-LMA. It should be pointed out that the computing platform for the CPU- and GPU-based GTA in this study is Core i7 6700k and GeForce GTX 1080ti, respectively. The GPU-GTA algorithm should be much faster on a better GPU workstation.

## V. CONCLUSION

A GPU-based grid traverse geolocation algorithm (GPU-GTA) for lightning location networks is proposed and examined. The overall performance of GPU-GTA is examined by applying it to JASA (a six-sensor 2-D lightning location network in central China) and LFI-LMA (a five-sensor 3-D LMA in Duke University). The results show that the GPU-GTA algorithm can be easily implemented in both 2-D and 3-D lightning geolocation networks or any other multi-station networks. The location accuracy of GPU-GTA is validated with Monte Carlo simulations. The results show that GPU-GTA can locate a lightning source with sufficient accuracy over the coverage of a network. The processing time of GPU-GTA to locate a lightning event is found to be 2700 times faster than that of CPU-GTA, making GPU-GTA efficient enough for locating a source in 3-D in real-time.

Moreover, GPU-GTA can give a more accurate lightning event location than the traditional one. As we know, most existing lightning location networks are based on real-time analytical solutions of certain simple models, whereas the reality is much more complicated. With GPU-GTA, for a given network, one can build up a database based on numerical solutions of certain complete models under various scenarios in advance, and the lightning event location can then be easily determined with the GTA in real time. For example, the earth ground is rough, and its topography always causes inherent propagation delay of the lightning electromagnetic pulse to sensors away from the lightning source. This kind of time delay can be easily predicted with FDTD wave simulation in advance and pre-input to the GTA database [47]. GPU-GTA can then take this pre-input time delay into account to get a more accurate lightning event location than the traditional one.

## REFERENCES

- [1] X.-M. Shao, M. Stanley, A. Regan, J. Harlin, M. Pongratz, and M. Stock, "Total lightning observations with the new and improved Los Alamos Sferic Array (LASA)," *J. Atmos. Ocean. Technol.*, vol. 23, no. 10, pp. 1273–1288, 2006.
- [2] D. Smith *et al.*, "The Los Alamos Sferic Array: A research tool for lightning investigations," *J. Geophys. Res., Atmos.*, vol. 107, no. D13, pp. ACL 5-1–ACL 5-14, 2002.
- [3] K. L. Cummins and M. J. Murphy, "An overview of lightning locating systems: History, techniques, and data uses, with an in-depth look at the US NLDN," *IEEE Trans. Electromagn. Compat.*, vol. 51, no. 3, pp. 499–518, Aug. 2009.
- [4] Y. Wang *et al.*, "Beijing lightning network (BLNET) and the observation on preliminary breakdown processes," *Atmos. Res.*, vol. 171, pp. 121–132, 2016.
- [5] C. Rodger *et al.*, "Detection efficiency of the VLF world-wide lightning location network (WWLLN): Initial case study," *Ann. Geophys.*, vol. 24, no. 12, pp. 3197–3214, 2006.
- [6] Z. Qin, B. Zhu, F. Lyu, M. Ma, and D. Ma, "Using time domain waveforms of return strokes to retrieve the daytime fluctuation of ionospheric D layer," (in Chinese), *Chin. Sci. Bull.*, vol. 60, no. 7, pp. 654–663, 2015.
- [7] H. D. Betz *et al.*, "LINET—An international lightning detection network in Europe," *Atmos. Res.*, vol. 91, no. 2, pp. 564–573, 2009.
- [8] J. Montanya, N. Pineda, V. March, A. Illa, D. Romero, and G. Solà, "Experimental evaluation of the Catalan lightning detection network," in *Proc. 19th Int. Lightning Detect. Conf.*, Tucson, AZ, USA, Apr. 24–25, 2006, pp. 1–7.
- [9] W. Koshak *et al.*, "North Alabama lightning mapping array (LMA): VHF source retrieval algorithm and error analyses," *J. Atmos. Ocean. Technol.*, vol. 21, no. 4, pp. 543–558, 2004.
- [10] C. A. Morales *et al.*, "Years of sferics timing and ranging NETWORK-STARNET: A lightning climatology over south america," in *Proc. 23rd Int. Lightning Detect. Conf./5th Int. Lightning Meteorol. Conf.*, 2014, pp. 271–350.
- [11] R. Said and M. Murphy, "GLD360 upgrade: Performance analysis and applications," in *Proc. 24th Int. Lightning Detect. Conf.*, CA, San Diego, USA, Apr. 18–21, 2016, pp. 1–8.
- [12] C. Liu and S. Heckman, "Using total lightning data in severe storm prediction: Global case study analysis from North America, Brazil and Australia," in *Proc. IEEE Int. Symp. Lightning Protection*, 2011, pp. 20–24.
- [13] K. L. Cummins, M. J. Murphy, E. A. Bardo, W. L. Hiscox, R. B. Pyle, and A. E. Pifer, "A combined TOA/MDF technology upgrade of the US National lightning detection network," *J. Geophys. Res., Atmos.*, vol. 103, no. D8, pp. 9035–9044, 1998.
- [14] S. J. Keogh, E. Hibbett, J. Nash, and J. Eyre, "The Met Office Arrival Time Difference (ATD) system for thunderstorm detection and lightning location," *Forecasting Res. Tech. Rep. 488*, Met Office, USA, Jun. 27, 2006.
- [15] K. Lagouvardos, V. Kotroni, H.-D. Betz, and K. Schmidt, "A comparison of lightning data provided by ZEUS and LINET networks over Western Europe," *Nat. Hazards Earth Syst. Sci.*, vol. 9, no. 5, pp. 1713–1717, 2009.
- [16] Z. Qin, B. Zhu, M. Chen, M. Ma, and D. Ma, "Configuration of a VLF/LF lightning detection network in central china and its application," *presented at the 9th Asia-Pacific Int. Conf. Lightning*, Nagoya, Japan, pp. 1–4, Jun. 2015.
- [17] F. Lyu *et al.*, "A low-frequency near-field interferometric-TOA 3-D lightning mapping array," *Geophys. Res. Lett.*, vol. 41, no. 22, pp. 7777–7784, 2014.
- [18] D. Shi *et al.*, "Low-frequency E-field detection array (LFEDA)—Construction and preliminary results," *Sci. China Earth Sci.*, vol. 60, no. 10, pp. 1896–1908, 2017.
- [19] W. Rison, R. J. Thomas, P. R. Krehbiel, T. Hamlin, and J. Harlin, "A GPS-based three-dimensional lightning mapping system: Initial observations in central New Mexico," *Geophys. Res. Lett.*, vol. 26, no. 23, pp. 3573–3576, 1999.
- [20] P. M. Bitzer *et al.*, "Characterization and applications of VLF/LF source locations from lightning using the Huntsville Alabama Marx Meter Array," *J. Geophys. Res.*, vol. 118, no. 8, pp. 3120–3138, 2013.
- [21] T. Wu, D. Wang, and N. Takagi, "Lightning mapping with an array of fast antennas," *Geophys. Res. Lett.*, vol. 45, no. 8, pp. 3698–3705, 2018.
- [22] D. E. Proctor, "A hyperbolic system for obtaining VHF radio pictures of lightning," *J. Geophys. Res.*, vol. 76, no. 6, pp. 1478–1489, 1971.
- [23] D. Boccippio, S. Heckman, and S. Goodman, "A diagnostic analysis of the Kennedy Space Center LDAR network: 1. Data characteristics," *J. Geophys. Res., Atmos.*, vol. 106, no. D5, pp. 4769–4786, 2001.
- [24] D. Boccippio, S. Heckman, and S. Goodman, "A diagnostic analysis of the Kennedy Space Center LDAR network: 2. Cross-sensor studies," *J. Geophys. Res., Atmos.*, vol. 106, no. D5, pp. 4787–4796, 2001.
- [25] R. J. Thomas *et al.*, "Accuracy of the lightning mapping array," *J. Geophys. Res., Atmos.*, vol. 109, no. D14207, pp. 1–34, 2004.
- [26] M. Qing, Z. Yijun, and H. Ping, "Lightning observation and field experiment with 3D SAFIR system during summer 2003 in Beijing-Hebei Area," in *Proc. 27th Int. Conf. Lightning Protection*, 2005, vol. 4, pp. 101–104.
- [27] E. Defer *et al.*, "Lightning activity for the July 10, 1996, storm during the stratosphere-troposphere experiment: Radiation, aerosol, and ozone-A (STERAO-A) experiment," *J. Geophys. Res., Atmos.*, vol. 106, no. D10, pp. 10151–10172, 2001.
- [28] P. Richard, A. Soulage, P. Laroche, and J. Appel, "The SAFIR lightning monitoring and warning system, applications to aerospace activities," in *Proc. Int. Aerosp. Ground Conf. Lightning Static Electricity*, Oklahoma City, NOAA, 1988, pp. 383–390.
- [29] W. J. Koshak and R. Solakiewicz, "TOA lightning location retrieval on spherical and oblate spheroidal earth geometries," *J. Atmos. Ocean. Technol.*, vol. 18, no. 2, pp. 187–199, 2001.

- [30] E. P. Krider, R. C. Noggle, and M. A. Uman, "A gated, wideband magnetic direction finder for lightning return strokes," *J. Appl. Meteorol.*, vol. 15, no. 3, pp. 301–306, 1976.
- [31] K. L. Cummins and M. J. Murphy, "An overview of lightning locating systems: History, techniques, and data uses, with an in-depth look at the US NLDN," *IEEE Trans. Electromagn. Compat.*, vol. 51, no. 3, pp. 499–518, Aug. 2009.
- [32] R. L. Dowden, J. B. Brundell, and C. Rodger, "VLF lightning location by time of group arrival (TOGA) at multiple sites," *J. Atmos. Solar-Terrestrial Phys.*, vol. 64, no. 7, pp. 817–830, 2002.
- [33] M. Akita, M. Stock, Z. Kawasaki, P. Krehbiel, W. Rison, and M. Stanley, "Data processing procedure using distribution of slopes of phase differences for broadband VHF interferometer," *J. Geophys. Res., Atmos.*, vol. 119, no. 10, pp. 6085–6104, 2014.
- [34] Z. Sun, X. Qie, M. Liu, D. Cao, and D. Wang, "Lightning VHF radiation location system based on short-baseline TDOA technique—Validation in rocket-triggered lightning," *Atmos. Res.*, vol. 129, pp. 58–66, 2013.
- [35] X.-M. Shao, P. Krehbiel, R. Thomas, and W. Rison, "Radio interferometric observations of cloud-to-ground lightning phenomena in Florida," *J. Geophys. Res., Atmos.*, vol. 100, no. D2, pp. 2749–2783, 1995.
- [36] X.-M. Shao, D. Holden, and C. Rhodes, "Broad band radio interferometry for lightning observations," *Geophys. Res. Lett.*, vol. 23, no. 15, pp. 1917–1920, 1996.
- [37] Z. Kawasaki, R. Mardiana, and T. Ushio, "Broadband and narrowband RF interferometers for lightning observations," *Geophys. Res. Lett.*, vol. 27, no. 19, pp. 3189–3192, 2000.
- [38] R. Mardiana and Z. Kawasaki, "Broadband radio interferometer utilizing a sequential triggering technique for locating fast-moving electromagnetic sources emitted from lightning," *IEEE Trans. Instrum. Meas.*, vol. 49, no. 2, pp. 376–381, Apr. 2000.
- [39] C. Rhodes, X. Shao, P. Krehbiel, R. Thomas, and C. Hayenga, "Observations of lightning phenomena using radio interferometry," *J. Geophys. Res., Atmos.*, vol. 99, no. D6, pp. 13059–13082, 1994.
- [40] M. Stock *et al.*, "Continuous broadband digital interferometry of lightning using a generalized cross-correlation algorithm," *J. Geophys. Res., Atmos.*, vol. 119, no. 6, pp. 3134–3165, 2014.
- [41] J.-Y. Lojou, M. J. Murphy, R. L. Holle, and N. W. Demetriades, "Nowcasting of thunderstorms using VHF measurements," in *Lightning: Principles, Instruments and Applications*. Berlin, Germany: Springer, 2009, pp. 253–270.
- [42] C. O. Hayenga and J. W. Warwick, "Two-dimensional interferometric positions of VHF lightning sources," *J. Geophys. Res., Oceans*, vol. 86, no. C8, pp. 7451–7462, 1981.
- [43] F. Lyu, S. A. Cummer, Z. Qin, and M. Chen, "Lightning initiation processes imaged with very high frequency broadband interferometry," *J. Geophys. Res., Atmos.*, vol. 124, pp. 1–11, 2019, doi: [10.1029/2018JD02981](https://doi.org/10.1029/2018JD02981).
- [44] Z. Qin, "The observation of ionospheric D-layer based on the multi-station lightning detection system," (in Chinese), Master degree dissertation, Earth and Space Science, Univ. Sci. Technol. China, Hefei, China, 2014.
- [45] N. Honma, K. L. Cummins, M. J. Murphy, A. E. Pifer, and T. Rogers, "Improved lightning locations in the Tohoku Region of Japan using propagation and waveform onset corrections," *IEEE Trans. Power Energy*, vol. 133, no. 2, pp. 195–202, 2013.
- [46] W. Schulz, G. Diendorfer, S. Pedebay, and D. R. Poelman, "The European lightning location system EUCLID—Part 1: Performance analysis and validation," *Nat. Hazards Earth Syst. Sci.*, vol. 16, no. 2, pp. 595–605, 2016.
- [47] T. Lu and M. Chen, "Modelling of effect of propagation of lightning electromagnetic pulse over rough ground," in *Proc. Asia-Pac. Int. Symp. Electromagn. Compat.*, 2016, vol. 1, pp. 155–157.
- [48] D. Li *et al.*, "On lightning electromagnetic field propagation along an irregular terrain," *IEEE Trans. Electromagn. Compat.*, vol. 58, no. 1, pp. 161–171, Feb. 2016.
- [49] D. Li, M. Rubinstein, F. Rachidi, G. Diendorfer, and W. Schulz, "Location accuracy evaluation of ToA-based lightning location systems over mountainous terrain," *J. Geophys. Res., Atmos.*, vol. 122, no. 21, pp. 11760–11775, 2017.
- [50] C. Nvidia, "Programming guide," 2010.
- [51] C. Nvidia, "Compute unified device architecture programming guide," 2007.
- [52] M. Harris, "Optimizing parallel reduction in CUDA," *NVIDIA Developer Technology*, vol. 2, p. 45, 2007.
- [53] F. Liu, Z. Qin, B. Zhu, M. Ma, M. Chen, and P. Shen, "Observations of ionospheric D layer fluctuations during sunrise and sunset by using time domain waveforms of lightning narrow bipolar events," (in Chinese), *Chin. J. Geophys.-Chin. Ed.*, vol. 61, no. 2, pp. 484–493, Feb. 2018.
- [54] Z. Qin, M. Chen, B. Zhu, and Y. P. Du, "An improved Ray theory and transfer matrix method-based model for lightning electromagnetic pulses propagating in Earth-ionosphere waveguide and its applications," *J. Geophys. Res., Atmos.*, vol. 122, pp. 712–727, 2017.
- [55] Z. Qin, M. Chen, and B. Zhu, "Study of earth-ionosphere waveguide effect on lightning pulse with Ray theory," in *Proc. 33rd Int. Conf. Lightning Protection*, 2016, pp. 1–5.
- [56] F. Liu *et al.*, "Observations of blue discharges associated with negative narrow bipolar events in active deep convection," (in English), *Geophys. Res. Lett.*, vol. 45, no. 6, pp. 2842–2851, Mar. 2018.
- [57] F. Lyu, S. A. Cummer, G. Lu, X. Zhou, and J. Weinert, "Imaging lightning intracloud initial stepped leaders by low-frequency interferometric lightning mapping array," *Geophys. Res. Lett.*, vol. 43, no. 10, pp. 5516–5523, 2016.



**Zilong Qin** (M'19) received the B.Eng. degree in IC design and integrated systems from Xidian University, Xidian, China, in 2010, the M.Sc. degree in atmospheric physics from the University of Science and Technology of China, Hefei, China, in 2014, and the Ph.D. degree in electrical engineering from The Hong Kong Polytechnic University, Hong Kong, in 2019.

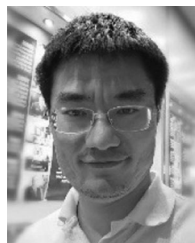
His main research interests include lightning detection technique, radio wave measurement instrument, wave modeling in earth ionosphere waveguide, and lower ionosphere probing technique. He is the

Principle Scientist in building the Jianghuai Area Sferic Array. Dr. Qin is a member of the American Geophysical Union.



**Mingli Chen** received the B.Sc. degree in physics from Lanzhou University, Lanzhou, China, in 1985, the M.Sc. degree in atmospheric physics from the Chinese Academy of Sciences, Beijing, China, in 1988, and the Ph.D. degree in electrical and electronic information from Gifu University, Gifu, Japan, in 2000.

From 1998 to 1996, he was a Researcher with the Lanzhou Institute of Plateau Atmospheric Physics, Chinese Academy of Sciences. He is currently a Professor with the Department of Building Services Engineering, The Hong Kong Polytechnic University, Hong Kong. His research interests include lightning physics, lightning detection, and structural lightning protection.



**Fanchao Lyu** (M'19) received the B.Eng. degree in communication engineering from Hohai University, Nanjing, China, in 2007, and the Ph.D. degree in natural science geophysics from the University of Science and Technology of China, Hefei, China, in 2013.

From 2013 to 2018, he was a Full-Time Postdoctoral Research Associate with the Department of Electrical and Computer Engineering, Duke University, Durham, NC, USA. He is currently a Research Fellow with the Department of Building Service Engineering, The Hong Kong Polytechnic University,

Hong Kong. His main research interests include lightning physics, development of radio emission measurement instrument and source location technique, as well as other fields relating to atmospheric electricity.

Dr. Lyu is a member of the American Geophysical Union.



**Steven A. Cummer** received the B.S., M.S., and Ph.D. degrees in electrical engineering from Stanford University, Stanford, CA, USA, in 1991, 1993, and 1997, respectively.

From 1997 to 1999, he was with the NASA Goddard Space Flight Center as a National Research Council Postdoctoral Research Associate. He is currently a Professor of electrical and computer engineering, Duke University, Durham, NC, USA. He has authored or coauthored more than 200 papers in refereed journals. His current research spans a variety of topics in complex materials for controlling electromagnetic and acoustic wave propagation and in geophysical remote sensing with a focus on lightning and atmospheric electricity.

Dr. Cummer is the recipient of a Presidential Early Career Award for Scientists and Engineers in 2001. He is a Fellow of the American Geophysical Union.



**Feifan Liu** received the B.Eng. degree in software engineering from Northwestern Polytechnic University, China, in 2014, and is currently working toward the Ph.D. degree in the area of lightning phenomenon and low ionosphere region at the University of Science and Technology of China, Hefei, China, China.

His main research interests include electrical discharge in earth's atmosphere such as the narrow bipolar events, blue jets, and their effects on near-earth space environments. He has participated in building the local lightning network of Jianghuai Area Sferic

Array (JASA), and is currently responsible for the routine maintenance and data analysis of the JASA.



**Baoyou Zhu** received the B.Eng. degree in atmospheric physics and environment and the Ph.D. degree both from the University of Science and Technology of China, Hefei, China, in 1995 and 2001, respectively.

In 2001, he joined the Department of Earth and Space Science, University of Science and Technology of China, as a Lecturer, and then became an Associate Professor in 2004. He is the Principle Investigator of Jianghuai Area Sferic Array. His main research interest include lightning meteorology and lightning

physics.

Dr. Zhu is a Life member of the Chinese Meteorological Society.



**Yaping Du** received the B.Sc. and M.Sc. degrees in electrical engineering from Shanghai Jiao Tong University, Shanghai, China, in 1984 and 1987, respectively, and the Ph.D. degree in electrical engineering from the University of Southern California, Los Angeles, CA, USA, in 1994.

He is currently a Professor with the Department of Building Services Engineering, The Hong Kong Polytechnic University, Hong Kong. His research interests include electromagnetic environments, lightning protection, and power quality in electric power

systems, electrified railway systems, and buildings.